

A new contribution for the impulsive synchronization of fractional-order discrete-time chaotic systems

Ouerdia Megherbi · Hamid Hamiche ·
Saïd Djennoune · Maamar Bettayeb

Received: 17 January 2017 / Accepted: 9 August 2017 / Published online: 20 August 2017
© Springer Science+Business Media B.V. 2017

Abstract In this paper, we discuss and investigate the impulsive synchronization of fractional-order discrete-time chaotic systems. The proposed method is based on the impulsive synchronization theory used in the integer-order case on the one hand and the mathematical analysis of the fractional-order discrete-time systems on the other hand. Sufficient conditions for the stability of synchronization error system are given, and application example with numerical simulations is illustrated in order to verify that the proposed method is applicable and effective. Furthermore, in order to validate the proposed synchronization approach, we have also provided the experimental implementation results using Arduino Mega boards.

Keywords Fractional-order systems · Chaotic systems · Impulsive synchronization · Delayed discrete-time systems · Lozi map · Arduino Mega boards

O. Megherbi (✉) · H. Hamiche · S. Djennoune
Laboratoire de Conception et Conduite des Systèmes de
Production (L2CSP), UMMTO, BP 17 RP, 15000
Tizi-Ouzou, Algeria
e-mail: meg_ouer@yahoo.fr

H. Hamiche
e-mail: hamid.hamiche07@gmail.com

S. Djennoune
e-mail: s_djennoune@yahoo.fr

M. Bettayeb
University of Sharjah, Sharjah, UAE
e-mail: maamar@sharjah.ac.ae

1 Introduction

Considered as a very interesting nonlinear phenomenon, Chaos has been intensively and widely studied in many fields of science and engineering over the last decades. In fact, it has been confirmed that the chaotic behavior can be present in some integer-order systems such as the Chua circuit [1], Liu system, Lü systems [2] and the Colpitts oscillator [3] as well as in fractional-order chaotic systems like the fractional-order Chen system [4], the fractional-order Lorenz system [5,6], the fractional-order financial system [7], the fractional-order Hénon maps [8,9] and the fractional-order logistic map [10].

The first successful initiative to synchronize two identical chaotic systems with different initial conditions was introduced by Pecora and Carroll [11], and the method was implanted on electronic circuits. Thanks to this interesting result, it has been possible to exploit the chaotic systems, thus synchronized, in different new interesting applications such as in the chaotic cryptography which means the secure transmission of data using the essential properties of the chaotic systems [12,13]. The synchronization techniques have been improved in recent years, and many different methods have been applied to synchronize chaotic systems. We can cite, for example, the projective synchronization [14], generalized synchronization [15], adaptive synchronization [16], and observer-based synchronization [17–19]. Another interesting method that has

known great growth, is the impulsive synchronization. In fact, this approach allows not only the synchronization of chaotic systems using small pulses generated by samples of the state variables of the driving system at discrete-time instances, but it offers also a direct method for digital modulation with chaotic carrier [20–25]. Recently, the study and the control of fractional-order chaotic systems have become a hot topic. On the basis of the recent results in the domain of the fractional calculus, whether in their modeling or their control, the impulsive synchronization and most of the above-cited synchronization approaches have been generalized to the fractional-order case [26–30]. Indeed, it has been shown that the fractional-order α can affect not only the chaotic behavior but also the synchronization performance [31]. For instance, in [32], the authors have noticed that the synchronization starts earlier for larger values of the derivative order α . Design of intelligent models and expert systems using artificial neural networks and neuro-fuzzy inference systems have been considered for modeling and implementing nonlinear chaotic systems in [33, 34], respectively. On the other hand, while studying the fractional-order networks, the authors of [35, 36] have both observed that lower and small fractional orders lead to better synchronization results. Furthermore, in the context of secure transmission, it should be emphasized that the use of fractional-order chaotic systems in secure communication schemes offers the advantage of improving the security level since the derivation orders act as additional secret keys [37]. One can also notice that, in comparison with the case of continuous chaotic systems, few studies have dealt with fractional-order discrete-time chaotic systems. Indeed, apart from some pioneer works such as [38–43], there is little progress made and results obtained in the fractional computation in discrete-time with respect to the continuous case. However, for the application in secure transmission of digital data, it is more practical and easier to use discrete systems than continuous ones since most of the proposed applications using analog systems have revealed serious difficulties to recover the message due to the channel noises [44]. In this paper, we exploit these results as well as the works carried out on the impulsive synchronization of integer-order chaotic systems to design, analyze and realize the impulsive synchronization scheme between two fractional-order discrete-time chaotic systems.

The paper is organized as follows: In Sect. 2, we, firstly, recall some preliminaries and concepts on fractional-order discrete-time systems, then we present and study the fractional-order chaotic Lozi map. In Sect. 3, we give some results of the impulsive synchronization obtained for the integer-order chaotic systems and we intend to use later. We discuss our contribution on the possibility of controlling two fractional-order discrete-time chaotic systems with the impulsive synchronization in Sect. 4. The obtained results are then applied on the fractional-order Lozi map. The synchronization scheme and simulation results are given in Sect. 5. The experimental implementation and results, using the Arduino Mega boards, are illustrated in Sects. 6 and 7, respectively. We end the paper with a conclusion and some interesting ideas for future works.

2 Fractional-order discrete-time chaotic systems

In this section, we, firstly, introduce some definitions from the discrete fractional calculus, and then, we consider one of them to model and study the dynamics of a fractional-order chaotic map.

2.1 Preliminaries on discrete fractional-order calculus

Several definitions of fractional derivatives and fractional integral have been proposed in the area of discrete fractional-order systems. The most used are Riemann–Liouville, Caputo, Grunwald–Letnikov formulas. Hereafter, we give a brief review of these different approaches to define fractional differences.

Definition 1 Let us define, at first, the set \mathbb{N}_a as $\mathbb{N}_a = \{a, a + 1, \dots\}$.

The α -order Caputo type difference is defined as follows: [45].

$$\begin{aligned} ({}_a\Delta_C^\alpha f)(t) &= ({}_a\Delta^{-(1-\alpha)}\Delta f)(t) \\ &= \frac{1}{\Gamma(1-\alpha)} \sum_{s=a}^{t-(1-\alpha)} (t-s-1)^{-\alpha} (\Delta f)(s), \end{aligned} \quad (1)$$

where $t \in \mathbb{N}_{a+(1-\alpha)}$, $\alpha \in (0, 1]$ and $f : \mathbb{N}_a \rightarrow \mathbb{R}$. The factorial function t^α is defined as follows:

$$t^\alpha = \frac{\Gamma(t+1)}{\Gamma(t+1-\alpha)}. \quad (2)$$

where Γ is the Euler gamma function

Definition 2 The α -order Riemann–Liouville difference is defined as follows [45]

$$(a\Delta_{RL}^\alpha f)(t) = \Delta(a\Delta^{-(1-\alpha)}\Delta f), \tag{3}$$

where $t \in \mathbb{N}_{a+(1-\alpha)}$, $\alpha \in (0, 1]$ and $f : \mathbb{N}_a \rightarrow \mathbb{R}$.

Let us present, now, the third definition we will use in the rest of this paper for modeling and synchronization of fractional-order chaotic maps.

Definition 3 The α -order Grunwald–Letnikov difference for a given state vector x is as follows [46]

$$\Delta^\alpha x(k) = \sum_{j=0}^k (-1)^j \binom{\alpha}{j} x(k-j), \tag{4}$$

where $\alpha > 0$ denotes the fractional order, $x(k) = [x_1(k) \ x_2(k) \ \dots \ x_n(k)] \in \mathbb{R}^n$ is the state vector at the current time, and $x(k-j)$ is the delayed state vector.

The term $\binom{\alpha}{j}$ can be computed from the following relation:

$$\binom{\alpha}{j} = \begin{cases} 1 & \text{for } j = 0, \\ \frac{\alpha(\alpha-1)\dots(\alpha-j+1)}{j!} & \text{for } j > 0, \end{cases} \tag{5}$$

To represent a fractional-order discrete-time system, let us consider, at first, the following integer discrete-time system [47]:

$$x(k+1) = f(x(k)), \tag{6}$$

where f is a smooth nonlinear function. We denote the 1-order difference for the discrete-time system (6) as:

$$\Delta^1 x(k+1) = x(k+1) - x(k) = f(x(k)) - x(k), \tag{7}$$

From (7), we define the α -order difference as [47]:

$$\Delta^\alpha x(k+1) = f(x(k)) - x(k), \tag{8}$$

Noting the α -difference (4), we obtain

$$\Delta^\alpha x(k+1) = x(k+1) - \alpha x(k) + \sum_{j=2}^{k+1} (-1)^j \binom{\alpha}{j} x(k-j+1), \tag{9}$$

We can introduce a new variable $p = j - 1$. Relation (9) becomes then:

$$\Delta^\alpha x(k+1) = x(k+1) - \alpha x(k) + \sum_{p=1}^k (-1)^{p+1} \binom{\alpha}{p+1} x(k-p), \tag{10}$$

By denoting the parameter $C_p = (-1)^{p+1} \binom{\alpha}{p+1}$ and substituting (10) into (8), we obtain the following relation :

$$x(k+1) = f(x(k)) + (\alpha - 1)x(k) - \sum_{p=1}^k C_p x(k-p). \tag{11}$$

Remark 1 We can note that if we set $\alpha = 1$ in (11), all the coefficients C_p , $p = 1, 2, \dots, k$ become 0. Therefore, by the definition of fractional-order difference, we can consider that an integer-order system is a special case of fractional-order systems.

Remark 2 In practical computing process, we cannot save all the states of a fractional-order discrete-time system since the great amount of calculation and the important space are needed for each computing iteration [48]. To resolve this problem, we can use a finite truncation to approximate a fractional-order discrete-time system. The truncation length, we denote by L , characterizes, in our case, a short memory and is often chosen appropriately and adapted to a practical problem.

Remark 3 Note that, for any selected derivative order, coefficients C_p decrease and vanish to 0 as the iteration number p increases. We can notice this in Fig. 1 which illustrates the computed coefficients C_p for different derivative orders values and for a memory length $L = 20$.

By applying this truncation to the fractional-order chaotic system (11), we get:

$$x(k+1) = f(x(k)) + (\alpha - 1)x(k) - \sum_{p=1}^L C_p x(k-p). \tag{12}$$

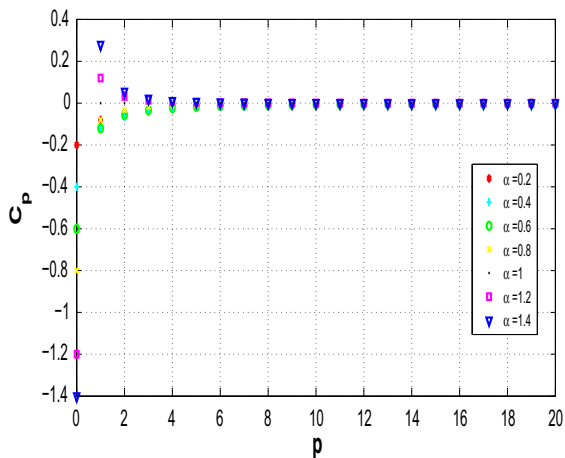


Fig. 1 C_p coefficients values for different derivative orders

Remark 4 Note that Eq. (12) is obtained in the commensurate case since the differentiation order α is supposed the same for all the state variables [49].

However, this is not always the case. To deal with the non-commensurate case, we should consider all the differentiation orders $\alpha_1, \alpha_2, \dots, \alpha_n$. The obtained model will be developed in Sect. 4 and will be used to describe a fractional-order discrete-time master system in the impulsive synchronization generalization for fractional-order case.

2.2 Fractional-order chaotic Lozi map

In this subsection, we aim to present an example of fractional-order discrete chaotic systems which is the fractional-order Lozi map and present some of its characteristics. The integer-order Lozi map is a two-dimensional discrete system [51]. Its state equations are given by:

$$\begin{cases} x_1(k + 1) = 1 - a |x_1(k)| + bx_2(k), \\ x_2(k + 1) = x_1(k), \end{cases} \tag{13}$$

where $[x_1 \ x_2]^T \in \mathbb{R}^2$ is the state vector and the parameters a and b are two constants. They satisfy the following conditions: $0 < b < 1$ and $1 + b < a < 2 - \frac{b}{2}$. We choose $a = 1.7$ and $b = 0.5$ so that the Lozi map presents a chaotic behavior.

The fractional discrete-time Lozi system is obtained by using the Grunwald–Letnikov approximation presented previously

$$\begin{cases} x_1(k + 1) = 1 - a |x_1(k)| + bx_2(k) + (\alpha_1 - 1)x_1(k) \\ \quad - \sum_{p=1}^L C_{p1}x_1(k - p) \\ x_2(k + 1) = x_1(k) + (\alpha_2 - 1)x_2(k) \\ \quad - \sum_{p=1}^L C_{p2}x_2(k - p), \end{cases} \tag{14}$$

where $0 \leq \alpha_1 \leq 1, 0 \leq \alpha_2 \leq 1$ are the derivative orders and the coefficients C_p are defined as follows: $C_{p1} = (-1)^{p+1} \binom{\alpha_1}{p+1}, C_{p2} = (-1)^{p+1} \binom{\alpha_2}{p+1}$.

Before using the fractional-order discrete-time Lozi system in the impulsive synchronization scheme, we should present some of its important characteristics, namely the sensitivity to initial conditions, the strange attractor, the bifurcation diagram and the Lyapunov exponents.

2.2.1 Sensitivity to initial condition

The sensitivity to the initial conditions is the fundamental characteristic allowing to recognize a chaotic behavior. It means that whatever the proximity of two initial states values, their trajectories rapidly diverge from each other. Figures 2 and 3 show, respectively, the effects of very small variations on the initial values of states x_1 and x_2 , of the fractional-order Lozi map, on their evolutions.

2.2.2 Strange attractor

Figure 4 shows the strange attractor of the fractional-order discrete-time Lozi system obtained by the phase plane of the state x_1 and x_2 . The derivative orders are taken as follows : $\alpha_1 = \alpha_2 = 0.95$. The selected initial conditions are $x_1(0) = 0.1$ and $x_2(0) = 0.2$.

2.2.3 Bifurcation diagram

The chaotic behavior of the fractional-order Lozi map can be seen from the bifurcation diagram illustrated in Fig. 5 and obtained by plotting one of the system states as a function of one control parameter (a in our case) while the second parameter is fixed. We can observe, on the diagram, the different behaviors of the Lozi map

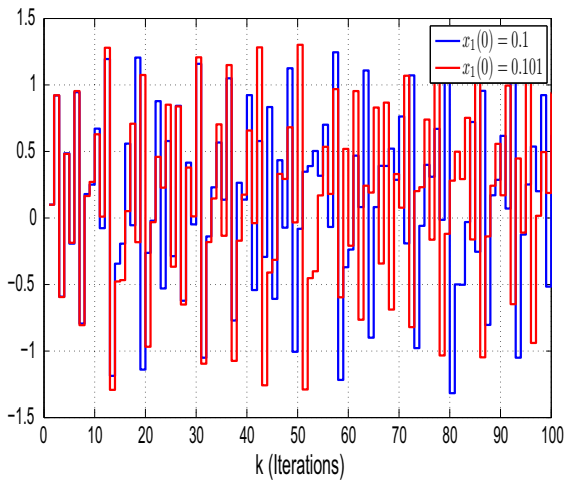


Fig. 2 Chaotic state x_1 evolutions for two close initial values

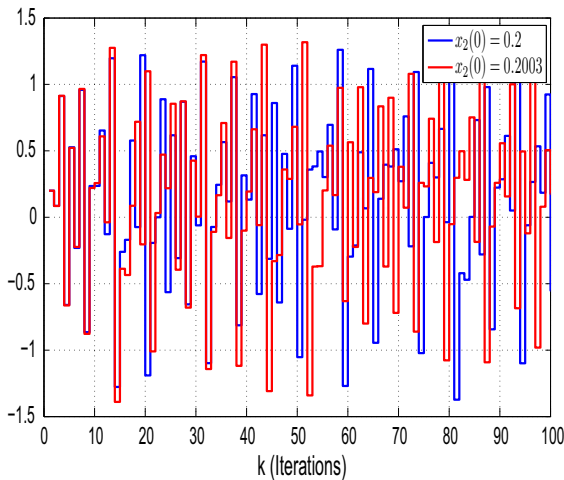


Fig. 3 Chaotic state x_2 evolutions for two close initial values

as the parameter a increases. Indeed, for low values of a , the evolution of x_1 is periodic. From $a \approx 0.55$, the number of periods begins to multiply by 2 until the chaos manifests at $a = 1.6$.

2.2.4 Lyapunov exponents

Figure 6 displays the Lyapunov exponents of the fractional-order Lozi map which are computed using MATLAB scripts. In order to simplify the calculation of Lyapunov exponents, we choose the size of memory $L = 1$, so the corresponding augmented system will present 4 Lyapunov exponents. The obtained values are : $\lambda_1 = 4.62589$, $\lambda_2 = -11.9961$, $\lambda_3 = -25.4058$,

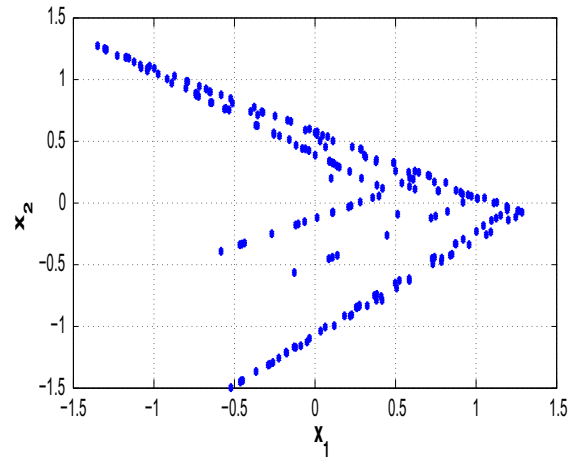


Fig. 4 Strange attractor of the fractional-order Lozi map with $a = 1.7$, $b = 0.5$ and $\alpha_1 = \alpha_2 = 0.95$

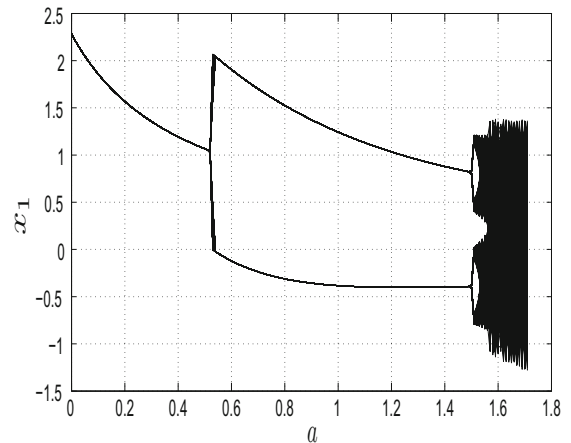


Fig. 5 Bifurcation diagram of the fractional-order Lozi map with $b = 0.5$ and $\alpha_1 = \alpha_2 = 0.95$.

$\lambda_4 = -42.0274$. We notice that one of the exponents is positive; this implies that the system is chaotic.

3 Impulsive synchronization of integer-order discrete-time chaotic systems

As mentioned above, the impulsive synchronization consists of the use of a pulses sequence in order to force a chaotic system to have the same behavior as another system [50]. To study this method, we consider the following master chaotic discrete-time system [51,52]:

$$x(k + 1) = Ax(k) + \varphi(x(k)), \tag{15}$$

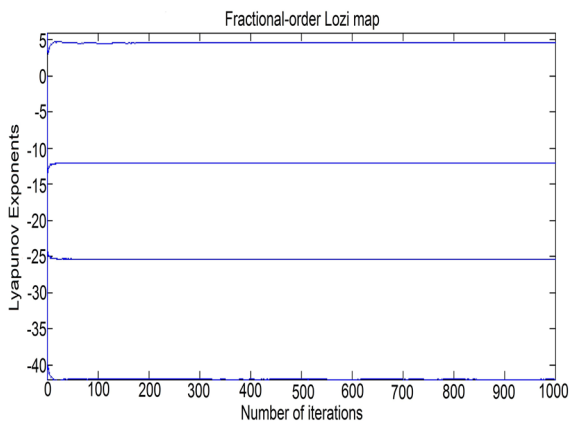


Fig. 6 Lyapunov exponents of the fractional-order Lozi map with $a = 1.7, b = 0.5$ and $\alpha_1 = \alpha_2 = 0.95$

where $x \in \mathbb{R}^n$ is the state vector and k is the discrete-time. $A \in \mathbb{R}^{n \times n}$ and $\varphi(x(k))$ is a n -dimensional non-linear map satisfying the Lipschitz condition:

$$\| \varphi(x(k)) - \varphi(\hat{x}(k)) \| < l \| x(k) - \hat{x}(k) \|, \tag{16}$$

where l is the Lipschitz constant and $\| \cdot \|$ denotes the standard Euclidian norm.

We define k_i as a subset of discrete-time k chosen so that $0 < 1 = k_1 < k_2, < \dots, < k_i < \dots, k_i \rightarrow \infty$ as $i \rightarrow \infty$. It denotes, in fact, the instants at which the pulses occur. In this paper, we assume that the pulses are periodic and denote the distance between two successive pulses by d . k_i^+ and k_i^- denote, respectively, the instants just after k_i and just before k_i . We can write this as follows:

$$k_i^+ = \lim_{\epsilon \rightarrow 0} k_i + \epsilon, \quad \epsilon > 0, \tag{17}$$

$$k_i^- = \lim_{\epsilon \rightarrow 0} k_i - \epsilon, \quad \epsilon > 0, \tag{18}$$

The response system of (15) is given by the following discrete-time impulsive observer:

$$\begin{cases} \hat{x}(k+1) = A\hat{x}(k) + \varphi(\hat{x}(k)) & \text{for } k \neq k_i, \\ \hat{x}(k_i^+) = \hat{x}(k_i) - B(k_i)e(k_i) & \text{for } k = k_i, i = 1, 2, \dots, \end{cases} \tag{19}$$

where $\hat{x} \in \mathbb{R}^n$ is the estimated state vector and $B(k_i), i = 1, 2, \dots$ are a sequence of $n \times n$ diagonal matrices. They are considered as control param-

eters and should be chosen appropriately to achieve synchronization.

The term $\hat{x}(k_i^-)$ is defined as follows : $\hat{x}(k_i^-) = \hat{x}(k_i)$. $e(k)$ is the synchronization error given by:

$$e(k) = x(k) - \hat{x}(k), \tag{20}$$

We define two further errors with respect to the instants k_i :

$$e(k_i^-) = x(k_i) - \hat{x}(k_i^-) = e(k_i), \tag{21}$$

$$e(k_i^+) = x(k_i) - \hat{x}(k_i^+), \tag{22}$$

The impulsive synchronization between systems (15) and (19) depends directly on the asymptotic stability of the following synchronization error [51]:

$$\begin{cases} e(k+1) = Ae(k) + \varphi(x(k)) - \varphi(\hat{x}(k)) & \text{for } k \neq k_i, \\ \Delta e(k) = e(k_i^+) - e(k_i^-) & \\ = B(k_i)e(k_i^-) = B(k_i)e(k) & \text{for } k = k_i \\ & i = 1, 2, \dots, \end{cases} \tag{23}$$

4 Impulsive synchronization of fractional-order discrete-time chaotic systems

In this section, we aim to extend the previous theory to impulsively synchronize two discrete-time fractional-order chaotic systems. The master system is defined as the system (12) obtained in Sect. 2, i.e.,

$$x(k+1) = f(x(k)) + (\alpha - 1)x(k) - \sum_{p=1}^L C_p x(k-p). \tag{24}$$

For a non-commensurate system (the derivative orders are different), we can rewrite the previous fractional-order difference equation as follows [49,53]:

$$x(k+1) = Ax(k) + \varphi(x(k)) - \sum_{p=1}^L A_d(p)x(k-p), \tag{25}$$

where the $n \times n$ matrix A describes the linear non-delayed part of the system and the vector $\varphi(x(k))$

denotes the nonlinear terms and satisfies the Lipchitz condition (16). $A_d(p)$ are diagonal $n \times n$ matrices which contain the coefficients C_p presented previously with respect to the derivative orders, namely:

$$A_d(p) = \begin{pmatrix} C_{p1} & 0 & \dots & 0 \\ 0 & C_{p2} & \dots & 0 \\ \vdots & \vdots & \ddots & \vdots \\ 0 & 0 & \dots & C_{pn} \end{pmatrix}.$$

The impulsive observer for system (25) is given by:

$$\begin{cases} \hat{x}(k+1) = A\hat{x}(k) + \varphi(\hat{x}(k)) \\ \quad - \sum_{p=1}^L A_d(p)\hat{x}(k-p), & \text{for } k \neq k_i, \\ \hat{x}(k_i^+) = \hat{x}(k_i) - B(k_i)e(k_i), & \text{for } k = k_i, \\ \quad i = 1, 2, \dots, \end{cases} \tag{26}$$

where $\hat{x} \in \mathbb{R}^n$ is the estimated state vector.

The synchronization error between the two systems is as follows:

$$\begin{cases} e(k+1) = Ae(k) + \tilde{\varphi}(x(k), \hat{x}(k)) \\ \quad - \sum_{p=1}^L A_d(p)e(k-p), \\ \quad \text{for } k \neq k_i \\ \Delta e(k) = B(k_i)e(k_i), \\ \quad \text{for } k = k_i, i = 1, 2, \dots, \end{cases} \tag{27}$$

with $\tilde{\varphi}(x(k), \hat{x}(k)) = \varphi(x(k)) - \varphi(\hat{x}(k))$.

We can notice, from (27), that the structure of the obtained system contains delayed terms. To study the impulsive synchronization between systems (25) and (26), we use the theorem developed earlier in [54], where the authors study the impulsive control of a delayed discrete system network.

Theorem 1 *Let λ be the largest singular value of A and γ the largest singular value of matrix A_α defined as follows:*

$$A_\alpha = \begin{pmatrix} \frac{\alpha_1 * (\alpha_1 - 1)}{2} & 0 & \dots & 0 \\ 0 & \frac{\alpha_2 * (\alpha_2 - 1)}{2} & \dots & 0 \\ \vdots & \vdots & \ddots & \vdots \\ 0 & 0 & \dots & \frac{\alpha_n * (\alpha_n - 1)}{2} \end{pmatrix}, \text{ where}$$

$\alpha_1, \alpha_2, \dots, \alpha_n$ are, respectively, the fractional derivative orders of states x_1, x_2, \dots, x_n .

If the following, Lipschitz relation is verified:

$$\|\varphi(x(k)) - \varphi(\hat{x}(k))\| < l \|x(k) - \hat{x}(k)\|,$$

and if there exist positive constants $q \leq 1$ and C defined as

$$C = \lambda + l + L \frac{\gamma}{q},$$

and satisfying the following condition:

$$\lim_{k \rightarrow \infty} C^k \|I + B(k_i)\|^i = 0,$$

then the error system (27) is asymptotically stable and systems (25) and (26) achieve the impulsive synchronization.

Proof For $k \neq k_i$, let us consider the following Lyapunov function

$$V(e(k)) = \|e(k)\|, \tag{28}$$

Then, we have

$$\begin{aligned} V(e(k+1)) &= \|e(k+1)\| \\ &\leq \|A\| \|e(k)\| + \|\tilde{\varphi}(x(k), \hat{x}(k))\| \\ &\quad + \sum_{p=1}^L \|A_d(p)\| \|e(k-p)\| \\ &\leq (\lambda + l) \|e(k)\| \\ &\quad + \|A_\alpha\| \sum_{p=1}^L \|e(k-p)\|. \end{aligned}$$

From Remark 3, we can deduce that

$$V(e(k+1)) \leq (\lambda + l)V(e(k)) + \gamma \sum_{p=1}^L V(e(k-p)), \tag{29}$$

if for any $p \in \mathbb{N}$, $qV(e(k-p)) \leq V(e(k))$ [55],

Then, by summing the delayed terms $V(e(k-p))$ from 1 to L , we obtain:

$$q \sum_{p=1}^L V(e(k-p)) \leq LV(e(k)), \tag{30}$$

If we multiply the last inequality by γ , we get

$$\gamma \sum_{p=1}^L V(e(k-p)) \leq \frac{L\gamma}{q} V(e(k)), \tag{31}$$

So, by replacing $\gamma \sum_{p=1}^L V(e(k-p))$ in Inequality (29), we can deduce that

$$V(e(k+1)) \leq \left(\lambda + l + \frac{L\gamma}{q}\right) V(e(k)), \tag{32}$$

This yields to

$$V(e(k)) \leq (\lambda + l + L \frac{\gamma}{q})V(e(k - 1)), \tag{33}$$

When $k = k_i$, we have

$$\begin{aligned} V(e(k_i^+)) &= \| I + B(k_i) \| \| e(k_i) \| \\ &= \| I + B(k_i) \| V(e(k_i)), \end{aligned} \tag{34}$$

By combining Inequality (33) and Inequality (34), and after successive iterations, we can write

$$\begin{cases} V(e(k)) \leq C^k \| I + B(k_i) \|^{i-1} V(e(0)) & \text{for } k_i \leq k \leq k_{i+1} \\ V(e(k_i^+)) \leq C^k \| I + B(k_i) \|^{i-1} V(e(0)) & \text{for } k = k_i \\ k = 1, 2, \dots, i = 1, 2, \dots \end{cases}, \tag{35}$$

where

$$C = \lambda + l + L \frac{\gamma}{q}. \tag{36}$$

From (35), we can notice that if the following relation is verified,

$$\lim_{k \rightarrow \infty} C^k \| I + B(k_i) \|^{i-1} = 0, \tag{37}$$

then the synchronization error system (27) is asymptotically stable for any initial condition $e(0)$, and the impulsive synchronization is achieved between systems (25) and (26). \square

Remark 5 Our main objective, in this paper, is to study the possibility of impulsive synchronization of two fractional-order discrete-time chaotic systems. This is why, we have not been interested in computing the maximum pulses period required to establish this synchronization.

5 Application to the impulsive synchronization of fractional-order Lozi maps

In this section, we consider as an illustrative example, the fractional-order Lozi map presented in Sect. 2. This section is divided into two parts: In the first one, we give the synchronization scheme and verify that conditions of Theorem 1 are well satisfied. In the second subsection, we give the obtained simulations results using MATLAB Script.

5.1 Impulsive synchronization scheme

The impulsive observer for system (14) is given by

$$\begin{cases} \hat{x}_1(k+1) = 1 - a | \hat{x}_1(k) | + b \hat{x}_2(k) + (\alpha_1 - 1) \hat{x}_1(k) \\ \quad - \sum_{p=1}^L C_{p1} \hat{x}_1(k-p) \\ \hat{x}_2(k+1) = \hat{x}_1(k) + (\alpha_2 - 1) \hat{x}_2(k) \\ \quad - \sum_{p=1}^L C_{p2} \hat{x}_2(k-p) & \text{for } k \neq k_i \\ \hat{x}(k_i^+) = \hat{x}(k_i) - B(k_i)e(k_i) & \text{for } k = k_i \end{cases}, \tag{38}$$

with $\hat{x} = [\hat{x}_1 \ \hat{x}_2] \in \mathbb{R}^n$ is the estimated state vector and the diagonal matrix $B(k_i)$ contains the control factors allowing the impulsive synchronization. The error system obtained between systems (14) and (38) can be written as follows

$$\begin{cases} e(k+1) = Ae(k) + \tilde{\varphi}(x(k), \hat{x}(k)) \\ \quad - \sum_{p=1}^L A_d(p)e(k-p), & \text{for } k \neq k_i \\ \Delta e(k) = B(k_i)e(k_i), & \text{for } k = k_i \end{cases}, \tag{39}$$

where $e = [e_1 \ e_2]^T \in \mathbb{R}^2$ is the error vector. The Lozi parameters are taken as presented in the previous section, namely $a = 1.7$ and $b = 0.5$.

In order to satisfy the condition of Theorem 1 presented in Sect. 4, the derivative orders are taken as follows: $\alpha_1 = 0.95$, $\alpha_2 = 0.95$ and the memory length is chosen as $L = 5$. Matrix A is then defined as:

$$A = \begin{pmatrix} \alpha_1 - 1 & b \\ 1 & \alpha_2 - 1 \end{pmatrix},$$

and the nonlinear map $\tilde{\varphi}(x(k), \hat{x}(k)) \in \mathbb{R}^2$ is obtained as follows:

$$\begin{aligned} \tilde{\varphi}(x(k), \hat{x}(k)) &= \begin{pmatrix} 1 - a | x(k) | - 1 + a | \hat{x}(k) | \\ 0 \end{pmatrix} \\ &= \begin{pmatrix} -a(| x(k) | - | \hat{x}(k) |) \\ 0 \end{pmatrix}, \end{aligned}$$

This implies that $\| \tilde{\varphi}(x(k), \hat{x}(k)) \| \leq a(\| x(k) \| - \| \hat{x}(k) \|)$. It is, then, easy to deduce that Lipschitz constant l is equal to the parameter a , namely $l = 1.7$. The matrices $A_d(p)$ for the fractional-order Lozi map are defined as

$$A_d(p) = \begin{pmatrix} C_{p1} & 0 \\ 0 & C_{p2} \end{pmatrix},$$

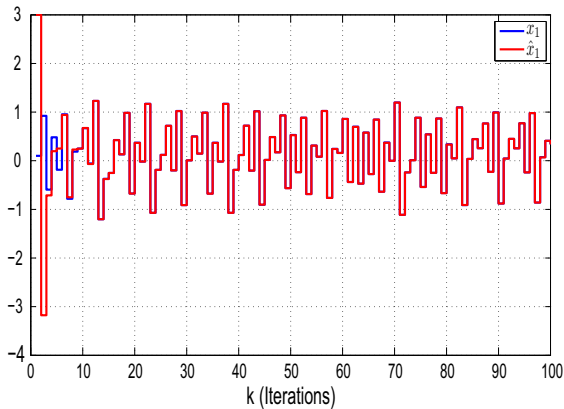


Fig. 7 Synchronized states x_1 and \hat{x}_1

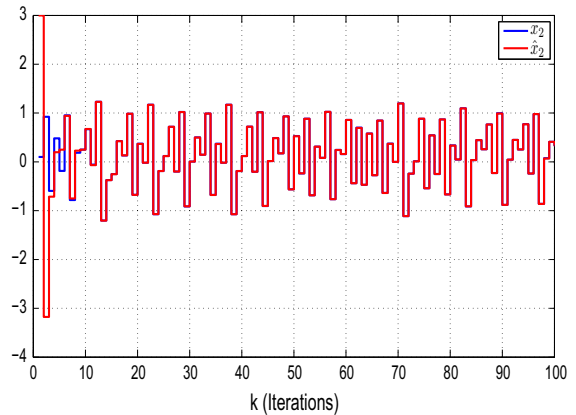


Fig. 8 Synchronized states x_2 and \hat{x}_2

For the above chosen parameters, we get the following numerical results $\lambda = \|A\| = 1.0050$, $\gamma = \|A_\alpha\| = 0.0238$, $q = 0.0408$.

The control signal is a pulse train of magnitude $M = 1$ and period $d = 3$, and the correction matrix B is also chosen constant and defined by

$$B = \begin{pmatrix} b_1 & 0 \\ 0 & b_2 \end{pmatrix} = \begin{pmatrix} -0.98 & 0 \\ 0 & -0.98 \end{pmatrix}.$$

The numerical results have shown that, for the above chosen parameters, $C^k \|I + B(k_i)\|^i \rightarrow 0$ as $k \rightarrow \infty$. In the following section, we provide the simulation results of the impulsive synchronization scheme described above.

5.2 Simulation results

This section provides the simulations results, achieved on MATLAB and obtained by applying the above theory to the fractional-order Lozi map to verify the effectiveness of the proposed synchronization method. The chosen initial conditions are $x_1(0) = 0.1$, $x_2(0) = 0.2$ for the master system and $\hat{x}_1(0) = 3$, $\hat{x}_2(0) = 2$ for the fractional-order impulsive observer.

We start with the synchronization results. Figures 7 and 8, respectively, show the synchronization between the states x_1, \hat{x}_1 and x_2, \hat{x}_2 of the Lozi map; we can see that the states of the Lozi map are well reconstructed at the receiver level by using the fractional-order impulsive observer designed in the previous section.

The synchronization errors illustrated in Figs. 9 and 10 show that errors converge to zero after a short number of iterations. This confirms the above results.

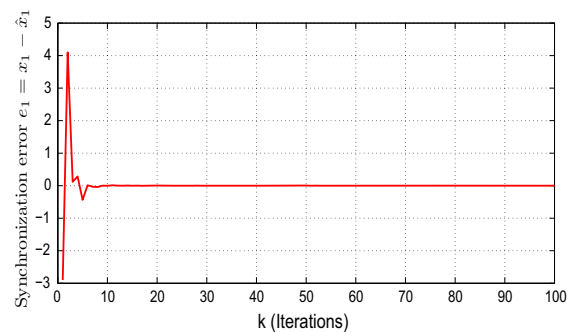


Fig. 9 Synchronization error $e_1 = x_1 - \hat{x}_1$

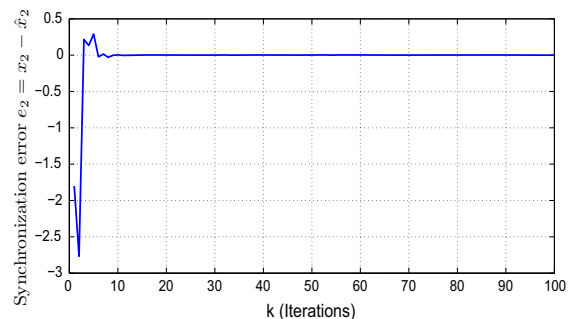


Fig. 10 Synchronization error $e_2 = x_2 - \hat{x}_2$

As mentioned in Sect. 5, chaotic systems are very sensitive to initial conditions. However and obviously, the synchronization should not be affected by this characteristic. To verify this, we have chosen different and dispersed initial values of the impulsive observer states and observed the variation effect on the synchronization process. Figure 11 shows the synchronization results for $(x_1(0), \hat{x}_1(0)) = (0.1, -17)$. We can see

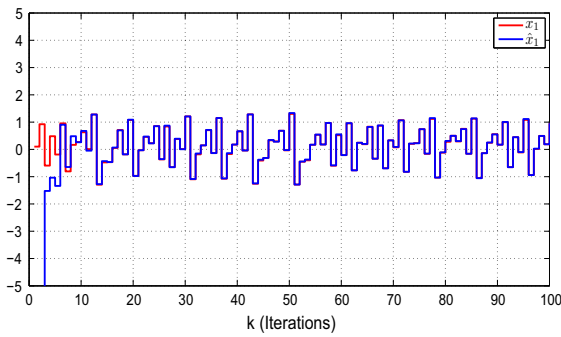


Fig. 11 Synchronized states x_1 and \hat{x}_1 for $\hat{x}_1(0) = -17$

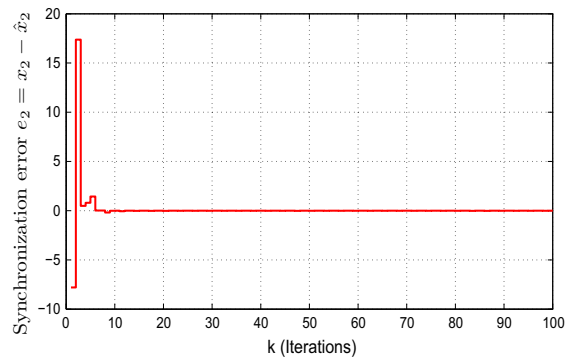


Fig. 14 Synchronization error $e_2 = x_2 - \hat{x}_2$ for $\hat{x}_2(0) = 8$

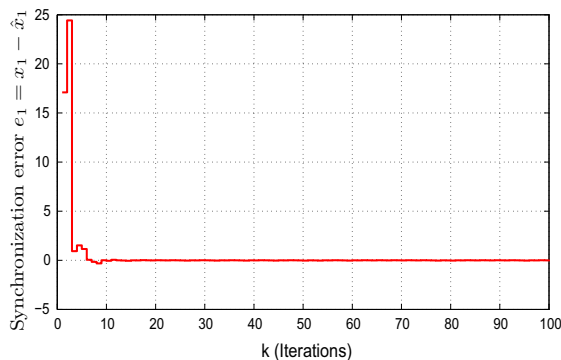


Fig. 12 Synchronization error $e_1 = x_1 - \hat{x}_1$ for $\hat{x}_1(0) = -17$

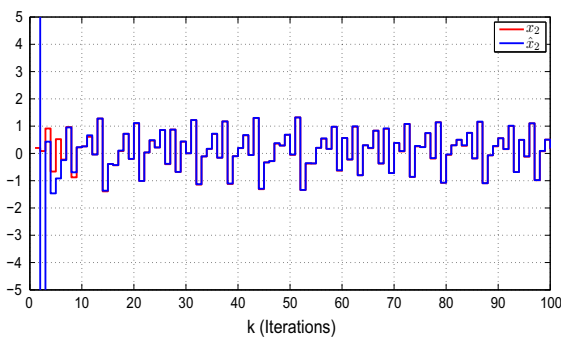


Fig. 13 Synchronized states x_2 and \hat{x}_2 for $\hat{x}_2(0) = 8$

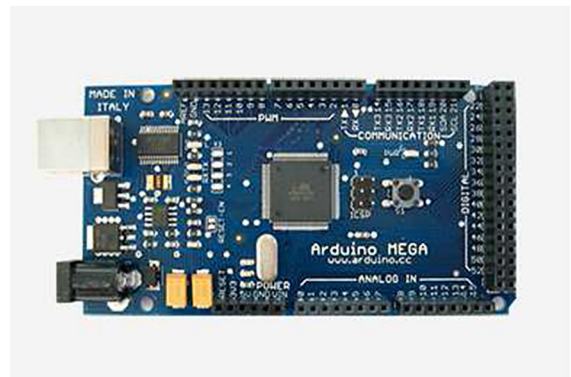


Fig. 15 Arduino Mega board

6 Experimental implementation of the impulsive synchronization

In this section, we develop in more details the practical implementation of the impulsive synchronization, applied on the fractional-order Lozi map, using the Arduino Mega boards.

The Arduino Mega board shown in Fig. 15 is a microcontroller board with open-source software and hardware[56]. Indeed, there exists a important range of different boards with different features on the market. However, they share a common feature which is easy to develop programs on them. Furthermore, Arduino Mega boards provide a free IDE in order to program the board and to help the user with writing, compiling and uploading codes into the boards. The essential component of the Arduino Mega board is the Atmel ATmega328 microcontroller; this latter is running at 16 MHz with a 8-bit core and a limited memory which consists of 32 kB of storage and 2 kB of random access memory [57]. Further, the Arduino Mega is equipped

that despite the large difference in the initial values of the observer state \hat{x}_1 , the impulsive synchronization is well established. The synchronization error illustrated in Fig. 12 confirms the above result since it converges to zero after a short number of iterations. From Figs. 13 and 14, we can make the same conclusion for the state x_2 . Indeed, The synchronization is still achieved even for $(x_2(0), \hat{x}_2(0)) = (0.2, 8)$.

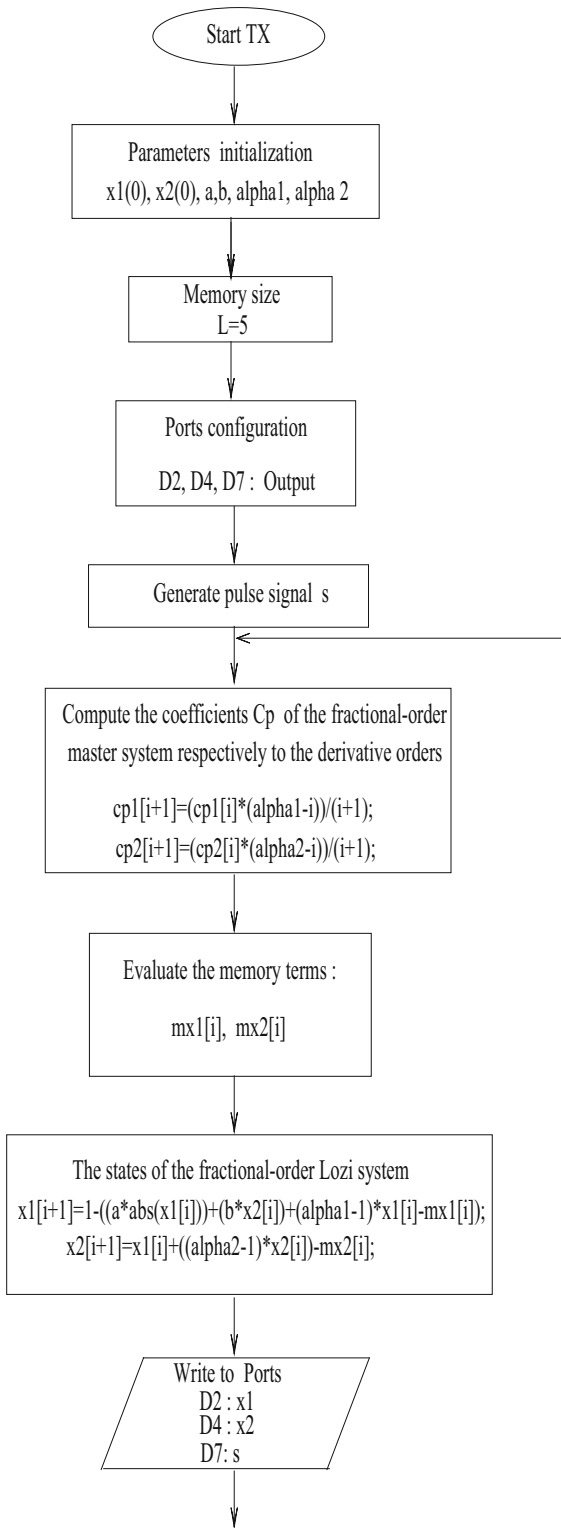


Fig. 16 Algorithm for the master fractional-order Lozi system

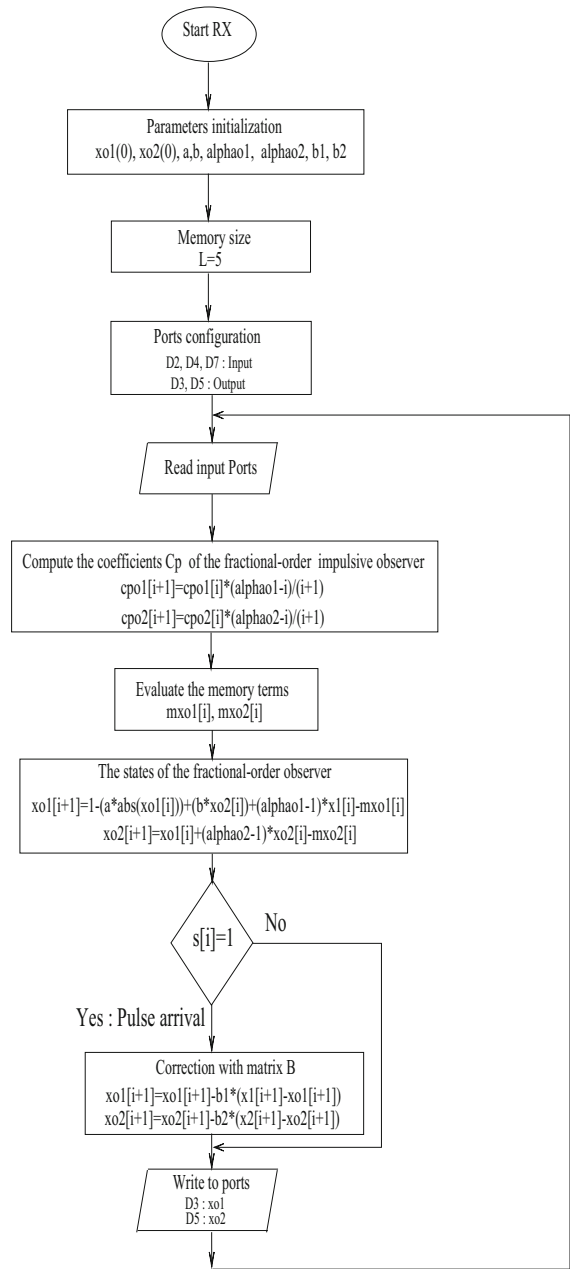


Fig. 17 Algorithm for the fractional-order impulsive observer

with 54 digital inputs/outputs, 16 analog inputs, 4 UARTs (hardware serial ports), a USB connection, a power jack, an ICSP header, and a reset button [58].

In our work, we have used two Arduino Mega boards: We have uploaded, using an USB cable, the Master fractional-order Lozi Map into the first Arduino Mega board and the fractional impulsive observer

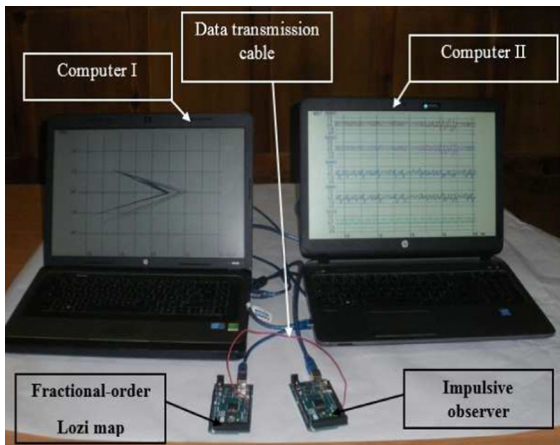


Fig. 18 Picture of the practical implementation

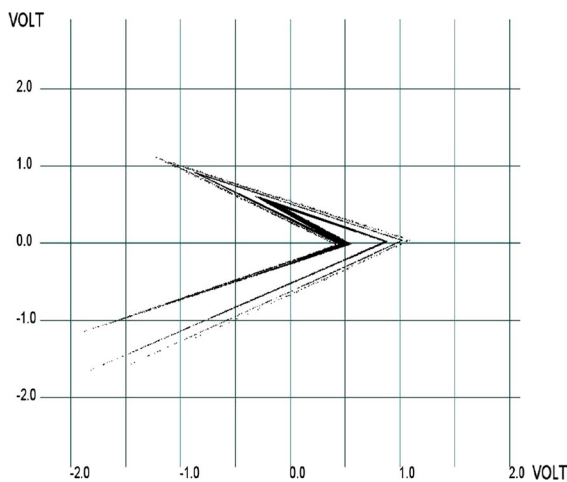


Fig. 19 Strange attractor of the chaotic fractional-order Lozi map using Arduino Mega board (x_2 vs. x_1)

code into the second Arduino board. The connection between the two boards is achieved by cable from the TX port of the first Arduino board (the master fractional-order Lozi map) and the RX port of the second Arduino board (the fractional-order impulsive observer). It should be known that data are coded on 8 bits and transmitted in serial way.

The codes uploaded into the two boards have been programmed using the language Wiring which is similar to the C Language. In order to facilitate the description of the synchronization scheme, the main algorithms executed by the Arduino boards are shown in Figs. 16 and 17.

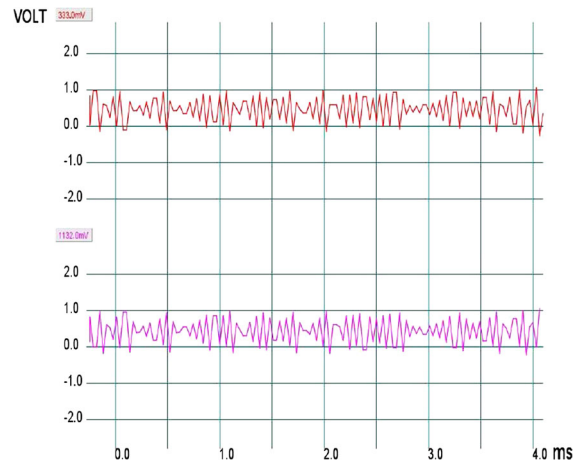


Fig. 20 States x_1 (upper signal) and x_2 (lower signal) of the fractional-order Lozi map

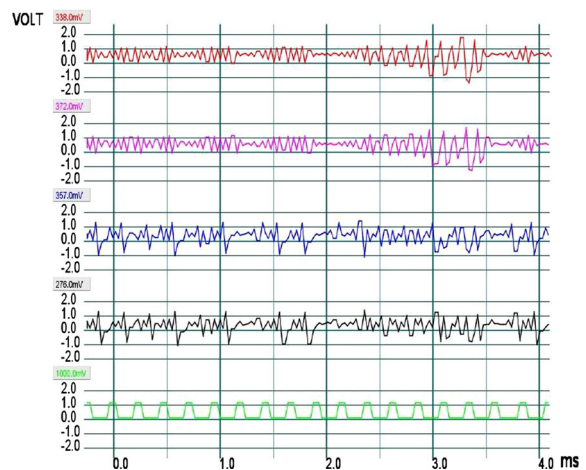


Fig. 21 Impulsive synchronization results : (from the upper) : state x_1 , state \hat{x}_1 , state x_2 , state \hat{x}_2 and the control pulses

In order to make the results visualization more easy and precise, instead of using a digital oscilloscope, we have used two individual computers each with a graphical interface written in Java. Figure 18 illustrates better both the Arduino Mega boards connection and the results displaying process.

7 Experimental results of the impulsive synchronization

We start the experimental results with Fig. 19 which illustrates the Lozi attractor, presented previously, using the Arduino Mega board.

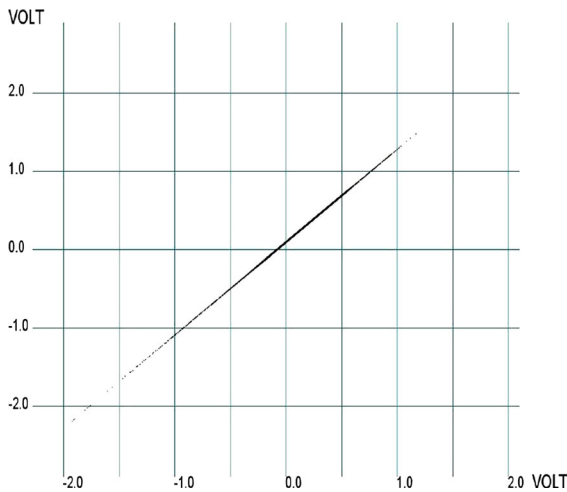


Fig. 22 Phase plane x_1 versus \hat{x}_1

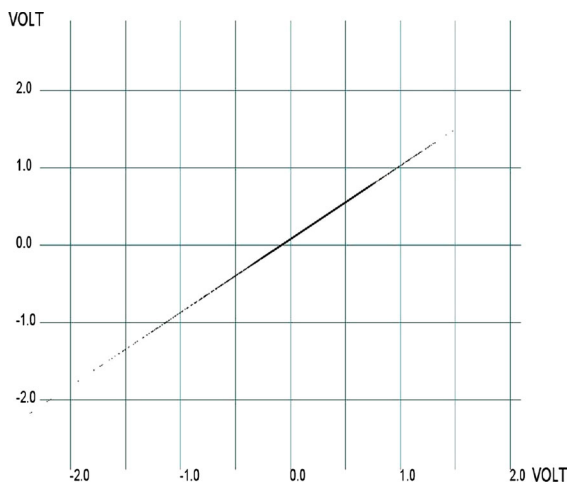


Fig. 23 Phase plane x_2 versus \hat{x}_2

The two states x_1 and x_2 of the fractional-order chaotic Lozi map are shown in Fig. 20. The upper signal presents the x_1 chaotic evolution and the lower signal the x_2 chaotic evolution.

The reconstruction of the chaotic Lozi states under the impulsive control is well achieved using the Arduino Mega board. Indeed, in Fig. 21, five signals are illustrated, the two upper signals represent the states x_1 and \hat{x}_1 of the Lozi map and the impulsive observer. The two lower signals show the states x_2 and \hat{x}_2 , and the last signal illustrates the control pulses used.

To better observe the effectiveness of the impulsive synchronization, Figs. 22 and 23 display, respectively, the phase planes of the states x_1 versus \hat{x}_1 and x_2 versus

\hat{x}_2 . The straight line obtained in each case confirms that synchronization occurs well.

8 Conclusion

Our contribution in this paper consists of the generalization of the impulsive synchronization method to the fractional-order discrete-time chaotic systems. Based on both theories of discrete-time fractional-order systems and the impulsive control, a stability theorem has been given. The simulation results show the effectiveness of the impulsive control to synchronize fractional-order chaotic systems. Furthermore, the experimental results obtained by the implementation of the impulsive control scheme on Arduino Mega boards confirm and validate the proposed synchronization scheme. As future works, we can propose to give an efficient result to compute the pulses period allowed to achieve synchronization. In addition, we can use the obtained results in the design of a secure data transmission scheme.

References

1. Chua, L.O., Koracev, I., Eckert, K., Itoh, M.: Experimental chaos synchronization in chua's circuit. *Int. J. Bifurc. Chaos* **2**, 705–708 (1992)
2. Vaidyanathan, S.: Hybrid synchronization of Liu and Lü chaotic systems via adaptative control. *Int. J. Adv. Inf. Technol. (IJAIT)* **1**(6), 13 (2011)
3. Maggio, G.M., Kennedy, M.P.: Experimental manifestations of chaos in the Colpitts oscillator. In: *ICECS Proceeding*, pp. 194–204 (1997)
4. Li, C., Chen, G.: Chaos in the fractional order Chen system and its control. *Chaos Soliton Fractals* **22**(3), 549–554 (2004)
5. Yu, Y., Li, H., Wang, S., Yu, J.: Dynamic analysis of a fractional-order Lorenz chaotic system. *Chaos Soliton Fractals* **42**(2), 1181–1189 (2009)
6. Luo, C., Wang, X.: Chaos in the fractional-order complex Lorenz system and its synchronization. *Nonlinear Dyn.* **71**(01), 241–257 (2013)
7. Cui, Z., Yu, P., Wen, Z.: Dynamical behaviors and chaos in a new fractional-order financial system. In: *5th International Workshop (IWCFTA) on Chaos Fractals Theories and Applications*, pp. 109–113 (2012)
8. Liu, Y.: Chaotic synchronization between linearly coupled discrete fractional Hénon maps. *Indian J. Phys.* **90**(03), 313–317 (2016)
9. Hu, T.: Discrete chaos in fractional Hénon map. *Appl. Math.* **5**(15), 2243–2248 (2014)

10. Wua, G.C., Baleanu, D.: Chaos synchronization of the discrete fractional logistic map. *Signal Process.* **102**, 96–99 (2014)
11. Pecora, L.M., Carroll, T.L.: Synchronization in chaotic systems. *Phys. Rev. Lett.* **64**(8), 821–824 (1990)
12. Hamiche, H., Guermah, S., Saddaoui, R., Hannoun, K., Laghrouche, M., Djennoune, S.: Analysis and implementation of a novel robust transmission scheme for private digital communications using Arduino Uno board. *Nonlinear Dyn.* **81**(4), 1921–1932 (2015)
13. Hamiche, H., Ghanes, M., Barbot, J.P., Kemih, K., Djennoune, S.: Hybrid dynamical systems for private digital communications. *Int. J. Model. Ident. Contr.* **20**(02), 99–113 (2013)
14. Mainieri, R., Rehace, J.: Projective synchronization in three-dimensional chaotic systems. *Phys. Rev. Lett.* **82**(15), 3042–3045 (1999)
15. Rulkov, N.F., Sushchik, M.M., Tsimring, L.S., Abarbanel, H.D.I.: Generalized synchronization of chaos in directionally coupled chaotic systems. *Phys. Rev. E* **51**, 980 (1995)
16. Loria, A., Panteley, E., Zavala, A.: Adaptive observers with persistency of excitation for synchronization of chaotic systems. *IEEE Trans. Circ. Syst. I Regul. Pap.* **56**(11), 2703–2716 (2009)
17. Nijmeijer, H., Mareels, I.M.Y.: An observer looks at synchronization. *IEEE Trans. Circuits Syst. I Fundam. Theory Appl.* **44**, 882–890 (1997)
18. Hamiche, H., Guermah, S., Djennoune, S., Kemih, K., Ghanes, M., Barbot, J.P.: Chaotic synchronization and secure communication via sliding-mode and impulsive observers. *Int. J. Model. Identif. Control.* **20**(4), 305–318 (2013)
19. Feng, Y., Zheng, J., Sun, L.: Chaos synchronization based on sliding mode observer. In: *Systems and Control in Aerospace and Astronautics*, pp. 1366–1373 (2006)
20. Yang, T., Chua, L.O.: Impulsive stabilization for control and synchronization of chaotic systems: theory and application to secure communication. *IEEE Trans. Circuits Syst. I Fundam. Theory Appl.* **44**(10), 976–988 (1997)
21. Megherbi, O., Guermah, S., Hamiche, H., Djennoune, S., Ghanes, M.: A novel transmission scheme based on impulsive synchronization of two Colpitts chaotic systems. In: *3rd International Conference on Systems and Control (ICSC'13)*, Algiers, Algeria (2013)
22. Hamiche, H., Kemih, K., Ghanes, M., Zhang, G., Djennoune, S.: Passive and impulsive synchronization of a new four-dimensional chaotic system. *Nonlinear Anal. Theory Methods Appl.* **74**(04), 1146–1154 (2011)
23. Li, Z., Fang, J., Zhang, W., Wang, X.: Delayed impulsive synchronization of discrete-time complex networks with distributed delays. *Int. J. Nonlinear Dyn. Chaos Eng. Syst.* **82**(04), 2081–2096 (2015)
24. Ji, Y., Liu, X., Ding, F.: New criteria for the robust impulsive synchronization of uncertain chaotic delayed nonlinear systems. *Int. J. Nonlinear Dyn. Chaos Eng. Syst.* **79**(01), 1–9 (2015)
25. Kadir, A., Aili, M., Sattar, M.: Color image encryption scheme using coupled hyper chaotic system with multiple impulse injections. *Int. J. Light Electron Opt.* **129**, 231–238 (2017)
26. Jie, F., Miao, Y., Tie-Dong, M.: Modified impulsive synchronization of fractional order hyperchaotic systems. *Chin. Phys. B* **20**(12), 120508 (2011)
27. Liu, J.G.: A novel study on the impulsive synchronization of fractional-order chaotic systems. *Chin. Phys. B* **22**(6), 060510 (2013)
28. Andrew, L.Y.T., Li, X.F., Chu, Y.D., Hui, Z.: A novel adaptive-impulsive synchronization of fractional-order chaotic systems. *Chin. Phys. B* **24**(10), 100502 (2015)
29. Muthukumar, P., Balasubramaniam, P., Ratnavelu, K.: Sliding mode control design for synchronization of fractional order chaotic systems and its application to a new cryptosystem. *Int. J. Dyn. Control* **5**(1), 115–123 (2017)
30. Wang, Q., Qi, D.L.: Synchronization for fractional order chaotic systems with uncertain parameters. *Int. J. Control Autom. Syst.* **14**(1), 211–216 (2016)
31. N'Doye, I., Darouach, M., Voos, H.: Observer-based approach for fractional-order chaotic synchronization and communication. In: *European Control Conference (ECC)*, Zurich, Switzerland (2013)
32. Bhalekar, S., Daftardar-Gejji, V.: Synchronization of different fractional-order chaotic systems using active control. *Commun. Nonlinear Sci. Numer. Simulat.* **15**(11), 3536–3546 (2010)
33. Tuntas, R.: A new intelligent hardware implementation based on field programmable gate array for chaotic systems. *Appl. Soft Comput.* **35**, 237–246 (2015)
34. Tuntas, R.: The modelling and analysis of nonlinear systems using a new expert system approach. *Iran. J. Sci. Technol. Trans. A Sci.* **38**, 365–372 (2014)
35. Tang, Y., Wang, Z., Fang, J.: Pinning control of fractional-order weighted complex networks. *Chaos* **19**, 013112 (2009)
36. Wu, X., Lai, D., Lu, H.: Generalized synchronization of the fractional-order chaos in weighted complex dynamical networks with nonidentical nodes. *Nonlinear Dyn.* **69**, 667–683 (2012)
37. Kassim, S., Hamiche, H., Djennoune, S., Bettayeb, M.: A novel secure image transmission scheme based on synchronization of fractional-order discrete-time hyperchaotic systems. *Nonlinear Dyn.* **88**(4), 2473–2489 (2017)
38. Miller, K.S., Ross, B.: Fractional difference calculus. In: *Proceedings of the International Symposium of the Univalent Functions, Fractional Calculus and their Applications*, Nihon University Koriyama, pp. 139–152 (1988)
39. Guermah, S., Bettayeb, M., Djennoune, S.: Controllability and the observability of linear discrete-time fractional-order systems. *Int. J. Appl. Math. Comput. Sci.* **18**, 213–222 (2008)
40. Podlubny, I.: *Fractional Differential Equations*. Academic Press, San Diego (1999)
41. Atici, F.M., Eloe, P.W.: Linear systems of fractional nabla difference equations. *Rocky Mt. J. Math.* **41**(02), 353–370 (2011)
42. Mozyrska, D.: Multiparameter fractional difference linear control systems. *Discrete Dyn. Nat. Soc.* **2014**, Article ID 183782, 8 pp (2014). doi:[10.1155/2014/183782](https://doi.org/10.1155/2014/183782)
43. Dzielinski, A., Sierociuk, D.: Stability of discrete fractional order state–space systems. *J. Vib. Control.* **14**(09–10), 1543–1556 (2008)

44. Feki, M., Robert, B., Gelle, G., Colas, M.: Secure digital communication using discrete-time chaos synchronization. *Chaos Solitons Fractals* **18**(4), 881–890 (2003)
45. Mozyrska, D., Pawluszewicz, E.: Local controllability of nonlinear discrete-time fractional order systems. *Bull. Pol. Acad. Tech.* **61**(01), 251–256 (2013)
46. Kilbas, A.A., Srivastava, H.M., Trujillo, J.J.: Theory and application of fractional differential equations. In: van Mill, J. (ed.) *North Holland Mathematics Studies*. Elsevier, Amsterdam (2006)
47. Hamiche, H., Kassim, S., Djennoune, S., Guermah, S., Lahdir, M., Bettayeb, M.: Secure data transmission scheme based on fractional-order discrete chaotic system. In: *International Conference on Control, Engineering and Information Technology (CEIT'2015)*, Tlemcen, Algeria (2015)
48. Liao, X., Gao, Z., Huang, H.: Synchronization control of fractional-order discrete-time chaotic systems. In: *European Control Conference (ECC)*, Zürich, Switzerland (2013)
49. Bettayeb, M., Djennoune, S., Guermah, S., Ghanes, M.: Structural properties of linear discrete-time fractional-order systems. In: *Proceedings of the International Federation of Automatic Control (IFAC)*, Seoul, Korea (July 2008)
50. Megherbi, O., Kassim, S., Hamiche, H., Djennoune, S.: A New robust hybrid transmission scheme based on the synchronization of discrete-time chaotic systems. In: *International Workshop on Cryptography and its Applications (IWCA'16)*, Oran, Algeria (2016)
51. Zheng, Y.A., Nyan, Y.B., Liu, Z.R.: Impulsive synchronization of discrete chaotic systems. *Chin. Phys. Lett.* **20**(2), 199–201 (2003)
52. Zheng, Y.I., Nian, Y.B., Liu, Z.R.: Impulsive control for the stabilization of discrete chaotic system. *Chin. Phys. B* **19**(9), 1251–1253 (2002)
53. Dzieliński, A., Sierociuk, D.: Adaptive feedback control of fractional order discrete-time state-space systems. In: *Proceedings of the 2005 International Conference on Computational Intelligence for Modelling, Control and Automation, and International Conference on Intelligent Agents, Web Technologies and Internet Commerce, (CIMCA-IAWTIC'05)*, Vienna, Austria (2005)
54. Liu, B., Marquez, H.J.: Uniform stability of discrete delay systems and synchronization of discrete delay dynamical networks via Razumikhin technique. *IEEE Trans. Circuits Syst. I Regul. Pap.* **55**(9), 2795–2805 (2008)
55. Hsien, T.L., Lee, C.H.: Exponential stability of discrete time uncertain systems with time-varying delay. *J. Frankl. Inst.* **332**(4), 479–489 (1995)
56. Hamiche, H., Megherbi, O., Kara, R., Saddaoui, R., Laghrouche, M., Djennoune, S.: A new implementation of an impulsive synchronization of two discrete-time hyperchaotic systems using Arduino-Uno boards. *Int. J. Model. Identif. Control* (2017). doi:[10.1504/IJMIC.2017.10006362](https://doi.org/10.1504/IJMIC.2017.10006362)
57. Pano-Azucena, A.D., Rangel-Magdaleno, J.J., Tlelo-Cuautle, E., Quintas-Valles, A.J.: Arduino-based chaotic secure communication system using multi-directional multi-scroll chaotic oscillators. *Nonlinear Dyn.* **87**(4), 2203–2217 (2017)
58. Arduino: www.arduino.cc